Carrageenan Based Hybrid Materials with Ionic-Liquids for Sustainable and Recyclable Printable Pressure Sensors

João P. Serra[1,2#], Nelson Pereira[1,3,#], Daniela M. Correia[1,4], Carmen R. Tubio[5], José Luis Vilas-Vilela[5,6], Carlos M. Costa[1,2,7*] and Senentxu Lanceros-Mendez[1,2,5,8*]

[#]J. P. S. and N. P. contributed equally to this paper

[1]Physics Centre of Minho and Porto Universities (CF-UM-UP), University of Minho 4710-057 Braga, Portugal

[2]Laboratory of Physics for Materials and Emergent Technologies, LapMET, University of Minho 4710-057 Braga, Portugal

[3]Algoritmi Center, Minho University, 4800-058 Guimarães, Portugal

[4]Centre of Chemistry, University of Trás-os-Montes e Alto Douro, 5000-801, Vila Real, Portugal

[5]BCMaterials, Basque Center for Materials, Applications and Nanostructures, UPV/EHU Science Park, 48940 Leioa, Spain

[6]Departamento de Química Física, Facultad de Ciencia y Tecnología, Universidad del País Vasco (UPV/EHU), 48940 Leioa, Spain

[7]Institute of Science and Innovation for Bio-Sustainability (IB-S), University of Minho, 4710-053 Braga, Portugal

[8]Ikerbasque, Basque Foundation for Science, 48013 Bilbao, Spain

[*]cmscosta@fisica.uminho.pt

[*]senentxu.lanceros@bcmaterials.net

KEYWORDS: Natural polymer; Carrageenan; Ionic Liquids; Smart materials.

ABSTRACT: In the scope of reducing the environmental impact of electronic systems (e-waste), increasingly implemented in the scope of the digitalization of society, this work reports on the development of a sustainable pressure sensor based on the combination of the natural polymer carrageenan and the ionic liquid (IL) 1-butyl-3-methylimidazolium tetrachloroferrate ([Bmim][$FeCl_4$]). Different IL contents were incorporated into the carrageenan matrix (10, 20 and 40 wt.%) in order to evaluate the influence of IL content in the final properties of the hybrid materials. No variations are induced in the chemical structure of carrageenan by the inclusion of the IL. On the other hand, the thermal stability of the polymer decreases with increasing IL content, as well as the Young Modulus that decreases from 748 MPa for pristine carrageenan to 437 MPa for the composite with 40 wt.% IL content. The ionic conductivity increases up to 8.74×10^{-9} S/cm for the sample comprising 40 wt.% of IL. The recyclability of the developed materials has been accessed and the potential of the blends for the development of printable pressure sensors demonstrated.

INTRODUCTION

Internet of Things (IoT) (also known as Internet of Everything or the Industrial Internet) is an internet-based system composed by physical objects that are embedded with electronics, software, sensors, actuators and connectivity which enable these objects to connect with other nearby objects [1-2]. IoT and its contribution to the digitalization of economy and society is having already an enormous impact on various industries including transportation, healthcare, or entertainment, among others [3-5].

Taking into account the implementation of a reliable and responsive network, the ubiquitous installation of sensors connected to the network will be a critical step for the even faster growth of the IoT concept [6]. In particular, pressure and deformation sensors are among the most required ones due to their widespread applicability [7], being based on different pressure sensing principles including piezoresistive, piezoelectric, triboelectric or capacitive, among others [8-9].

Piezoresistive sensors allow to transduce an external pressure or deformation into an electrical resistance variation and are typically characterized by high adaptability, simple manufacturing and low energy consumption [10]. Most recently, piezoresistive sensors hold great promise in the scope of artificial intelligence, robotics and human computer interfaces, among others [11-13], placing new requirements in terms of flexibility, sensing area or performance with respect to the traditional solutions. Traditionally, piezoresistive sensors are based on strain gages and metallic semiconductors, the ones based on semiconductors materials showing high gauge factors (GF) -value that quantifies the resistance variation with deformation- but being mechanically fragile and difficult to implement in large areas or curved surfaces [14]. To address those issues, piezoresistive sensors are being developed using polymer composites that result from the combination of a polymer matrix with conductive fillers [10].

Piezoresistive sensors based on polymer composites are composed of different polymer matrices, including thermoplastic, cross-linkable UV polymers, elastomers and conductive polymers, blended with different fillers such as carbon nanotubes (CNTs), graphene, or silver nanowires, and lead to GF values ranging from 4 to ~ 130 with excellent mechanical properties [15-17].

Most of the polymer based piezoresistive sensors mentioned above are of synthetic origin and difficult to recycle and reuse at the end of their life. Thus, as the number of these sensors and their increasing use in the scope of the IoT will bring negative environmental consequences.

Recently a novel approach has been introduced based on the use of ionic liquids (ILs) as conductive fillers. ILs are commonly defined as molten salts composed by an organic cation and inorganic anions [18]. ILs present high electrochemical stability, non-flammability, low volatility, low vapor pressure, easy miscibility and high ionic conductivity [19], allowing to tune polymer properties and/or introduce new functionalities [20]. In particular, a new sensitive sensor concept, the piezoionic, has been introduced through the combination of a thermoplastic elastomer styrene-ethylene-butylene-styrene (SEBS) with the IL 1-butyl-3-methylimidazolium dicyanamide ([Bmim][$N(CN)_2$]), allowing the development of a pressure sensor with suitable response under loading and unloading compressive cycles with applied forces up to 10 N with sensitivity of 25 $k\Omega\ N^{-1}$ [21].

In addition, considering environmental, sustainable and economic issues, there is an increasing trend in the development of bio-based sensors for monitoring various physical-chemical conditions [22]. A bio-sensor based on Fe_3O_4/chitosan nanocomposites has been developed to detect gallic acid (GA), with a detection limit of 12.1 nM in a wide range from 0.5 to 300.0 μM with high recovery percentage (98% to 112.8) [23]. Also, a bio-based

sensor to measure human motion has been developed based on polyacrylamide-sodium casein-carboxymethyl chitosan (PAAM-SC-CC) with excellent mechanical characteristics- Further, its suitability for the monitoring of different human movement such as throat movement and joint extension as demonstrated[24].

Based on the former approaches and, in particular, attending to the sustainability paradigms, this work reports on the development of a pressure sensor based on the piezoionic effect by combining a natural polymer, carrageenan, and the IL 1-butyl-3-methylimidazolium tetrachloroferrate ([Bmim][$FeCl_4$]).

Carrageenan is a sulphated galactans linear polymer extracted from a red marine algae (Rhodophyta), composed by x-D-galactopyranose linked in different carbons (3 or 4 for β or α types) or with 3,6-anhydro-α-d-galactopyranose. There are different types of carrageenan: kappa (κ-), iota (ι-) and lambda (λ-), with different percentage of sulphate groups and 3,6-anydrogalactose ring. The most common carrageenan types used for application are iota and kappa [25], which have been implemented in the cosmetics, pharmaceuticals, food and electronic industries as primary proton battery [26] and dye-sensitized solar cell (DSSC) [27].

Due to their interesting characteristics which include their high abundance in nature, low cost and biodegradability, carrageenan emerges as an environmentally friendly material to be applied in electronic devices [28-29]. For this purpose, the major limitation is carrageenan low electrical conductivity, which can be overcome by using ILs. In this context, this work presents the development of an environmentally friendly pressure sensor based on the combination of carrageenan and different contents of the IL [Bmim][$FeCl_4$]. The specific IL was selected based on highly stable and non-volatile liquid [30]. The influence of IL content into the morphological, physical-chemical, thermal, mechanical and ionic conductivity was evaluated and the potential of the developed

blends to be applied as printable pressure sensors demonstrated, together with its recyclability.

EXPERIMENTAL

Materials

Carrageenan (iota-ι type) was purchased from Alfa Aesar and the IL 1-butyl-3-methylimidazolium tetrachloroferrate (III) >97% [Bmim][$FeCl_4$] was supplied by Iolitec. The [Bmim][$FeCl_4$] IL is characterized by a melting temperature < 20 ºC, viscosity of 43.4 cP and ionic conductivity of 4.37 $mS.cm^{-1}$.

Neat and [Bmim][$FeCl_4$]/Carrageenan films preparation

Neat carrageenan films were prepared after polymer dissolution in ultrapure water (ratio of polymer/ ultra-pure water of 3/97 wt.%.) under magnetic stirring at 50 ºC. For the processing of the [Bmim][$FeCl_4$]/carrageenan blends, different contents of the IL [Bmim][$FeCl_4$] (10, 20 and 40 wt.%) in relation to the polymer content were first dispersed in ultrapure water during 10 minutes, under magnetic stirring at 50 ºC. Subsequently, carrageenan was added to the solution (3/97 wt.%.) and magnetically stirred at 50 ºC. After the complete polymer dissolution, the solution was spread on petri dishes followed by solvent evaporation at room temperature for approximately 7 days until the samples dried (Figure 1a). Samples with an average thickness of 100 μm were obtained.

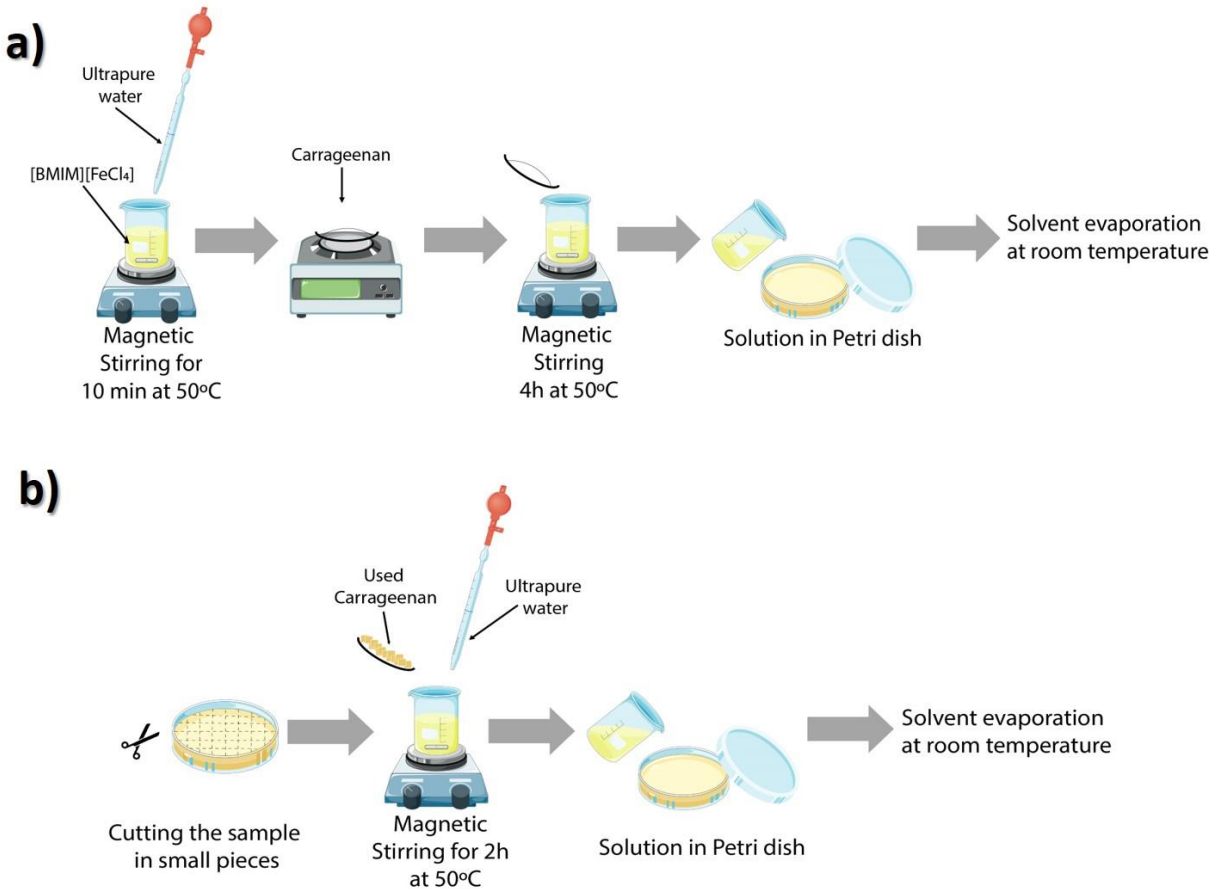

Figure 1. Schematic representation of the procedure used for the processing of the [Bmim][$FeCl_4$]/Carrageenan blends (a) and for the recycling of the blends (b).

Recycling and reuse of carrageenan films

In order to evaluate the possibility to reuse the previously developed IL/carrageenan blends, the samples were cut into small pieces of 5x5 mm and dissolved in ultrapure water at 50 °C under magnetic stirring. After complete dissolution, the sample was dispersed in a Petri dish and allowed to dry at room temperature (Figure 1b).

Samples characterization

The morphology of the samples was analysed by scanning electron microscopy (SEM, Zeiss EVO 40) with an accelerating voltage of 20 kV. Prior the analysis, the samples were

coated with a gold layer by magnetron sputtering with a Polaron, model SC502. Energy-dispersive X-ray (EDX) analysis was carried out with a Hitachi Tabletop Microscope TM 3000 apparatus to evaluate IL distribution within the sample. The vibration bands of the samples were obtained by Fourier Transformed Infrared Spectroscopy (FTIR) in the Attenuated Total Reflection mode (Jasco FT/IR-6100) from 4000 to 600 cm^{-1} after 64 scans at a resolution of 4 cm^{-1}. The thermal behaviour of the blends was analysed by both Differential Scanning Calorimetry (DSC) and Thermogravimetric analysis (TGA). DSC measurements were performed with a 822e Metler Toledo under nitrogen atmosphere in the temperature range between 25 ºC and 200 ºC at 10 °C.min^{-1}. The TGA measurements were carried out in a SDT-Q600 TGA apparatus (TA Instruments) between 25 ºC and 800 ºC, at 10ºC.min^{-1} under a nitrogen atmosphere.

The mechanical properties of the samples were evaluated by stress-strain tensile tests at room temperature in a TST350 Linkam Instrument set up at a strain rate of 15 $\mu m.s^{-1}$.

The ionic conductivity of the samples was measured with an Autolab PGSTAT-12 at frequencies from 1Hz to 65kHz in the temperature range between 20 and 95 ºC. The sample was placed between 2 gold electrodes of 10 mm diameter and placed inside a Buchi TO50 oven. The real and imaginary components of the impedance were obtained and the resistance R of the samples was obtained through the intercept of the imaginary impedance (minimum value of Z'') with the slanted line in the real impedance (Z'). The ionic conductivity was determined after equation 1:

$$\sigma = \frac{t}{A * R} \quad (1)$$

where t is the thickness and A the area of electrodes.

Piezoresistive pressure sensor functional demonstration, readout electronics and data acquisition system

A 5x5 piezoresistive sensor matrix was assembled with overall dimensions of 50 mm x 50 mm. Five silver electrodes (conductive silver nanoparticle ink Metalon HPS-021LV from Novacentrix) (Figure 2a-c) were screen printed using a semi-automatic printing equipment, model DX-305D from DSTAR on polyethylene terephthalate (PET) films (Melinex 506) with a polyester screen with 100 threads per centimeter. The dimensions of the digits of the electrodes were 50 mm × 50 mm as shown in Figure 2b).

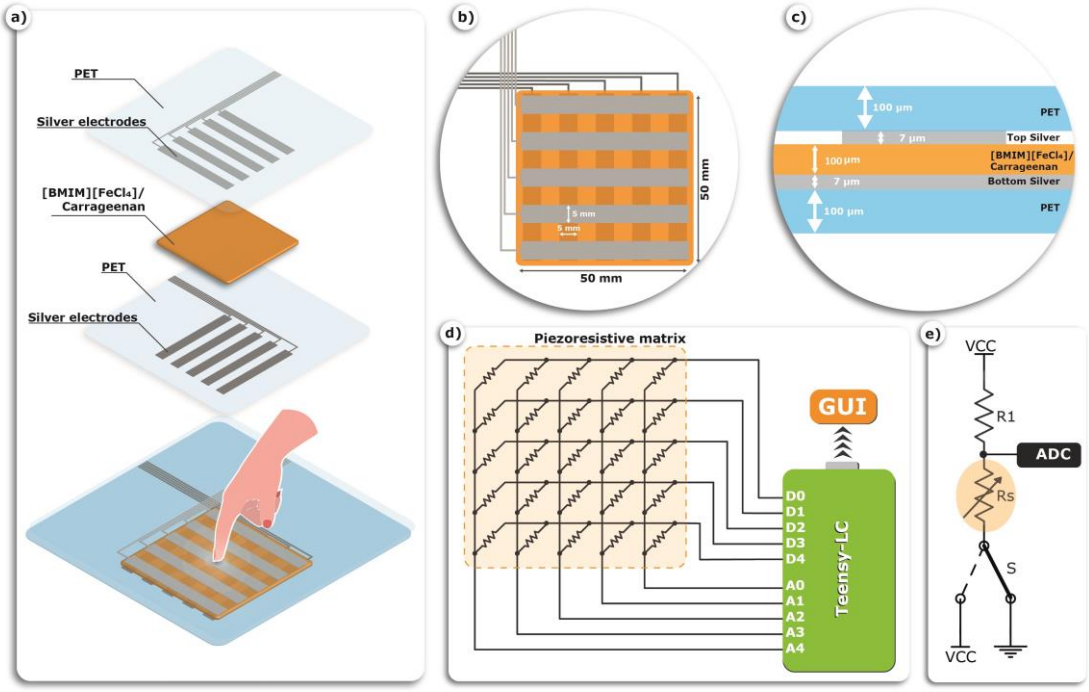

Figure 2. a) Diagram of the assembly process, b-c) details of the piezoresistive sensor with dimensions and thickness. d) Schematic representation of the connection of the piezoresistive matrix to the microcontroller. e) Detail of the algorithm for the readout of a sensor.

The piezoresistive film based on the [Bmim][$FeCl_4$]/Carrageenan with 40 wt.% IL sample was deposited on top of one of the electrodes and sandwiched together with the printed electrodes with double-side tape (3M), leaving the active material with some degree of freedom as shown in Figure 2c) with the corresponding thickness values. The freedom of the film allows the presence of some air (air gap) in the interface of the piezoresistive film with the printed silver electrodes, increasing the initial resistance of the sensors. The interface is reduced when a pressure is applied to the matrix resulting in the reduction of the initial resistance of the matrix sensors, the resistance being inversely proportional to the applied pressure. The connection with the electronic acquisition system was carried out by attaching 1 mm pitch flexible flat cable with 5 pins to the screen-printed electrodes using a z-axis conductive tape from 3M (9703).

The electronic acquisition system directly connects the piezoresistive matrix to a microcontroller. The microcontroller, Teensy-LC from PJRC, initially configures the internal pull-up resistors (R1 in figure 2e) of the 12 bits analog-to-digital converter (ADC) pins, allowing the readout of the sensors in the piezoresistive matrix through a voltage divider as shown in Figure 2d) and e). The microcontroller eliminates ghost points, when two or more detection points are in the active area, by connecting all except the readout line (E.g., D1-D4 to VCC) to the positive voltage (VCC), and the readout line (E.g., D0) to ground, forming the voltage divider. The output voltage of the voltage divider is them read by the ADC for all the columns (A0 to A4). The acquired data are them filtered for smooth visualization by a digital second order low pass Butterworth infinite impulse response (IIR) filter with a cut-out frequency of 10 Hz, increasing the stability and removing environment noise. Finally, the data is fed through a Universal Serial Bus (USB) to the computer for data visualization in a graphical user interface (GUI) built in python.

RESULTS AND DISCUSSION

Morphology

The morphology of neat carrageenan and the different [Bmim][$FeCl_4$]/carrageenan blends was analysed by SEM, as shown in the representative cross-section images of Figure 3. Neat carrageenan presents a layered and non-porous structure, ascribed to its semicrystalline structure [31]. Upon IL incorporation (10 and 20 wt.%) into the polymer matrix, the non-porous structure is preserved but becomes more compact due to the good distribution of the IL within the matrix (Figures 3b and 3c). The incorporation of and IL content of 40 wt.% (Figure 3d), on the other hand, induces an increase in the sample roughness, which may be attributed to phase segregation of the IL within the polymer matrix, exceeding IL being located on the surface of the blend [32].

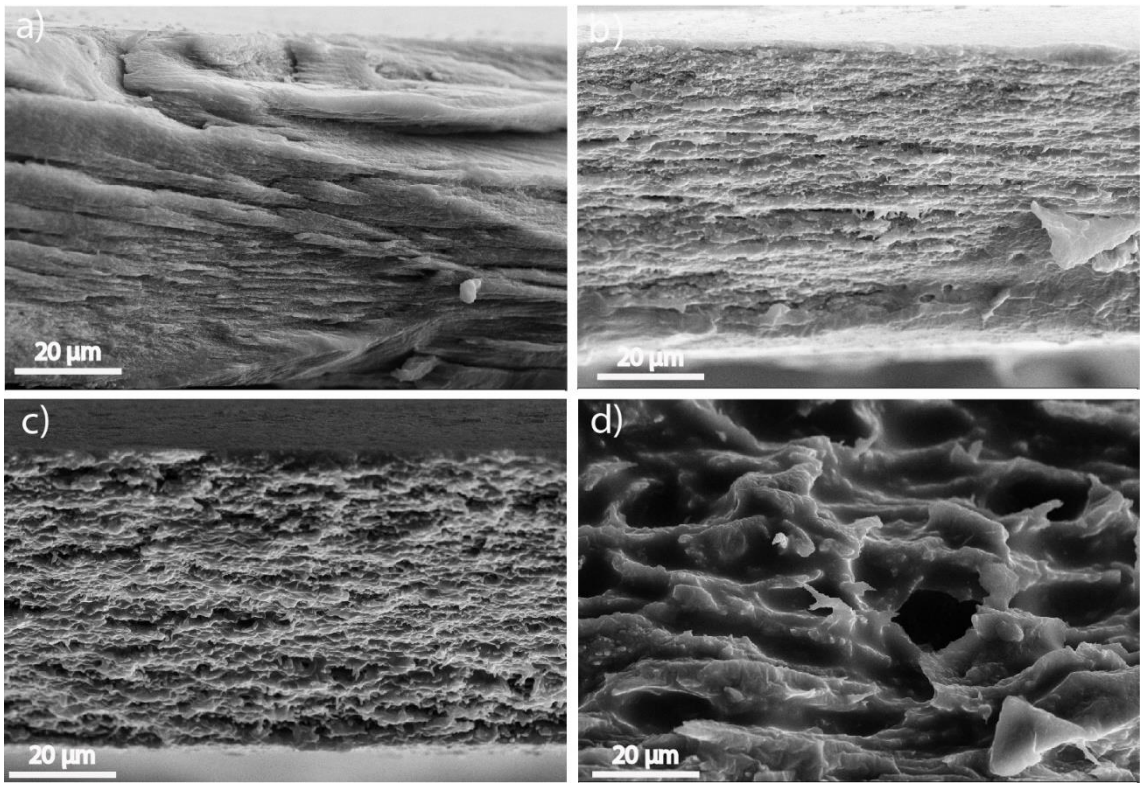

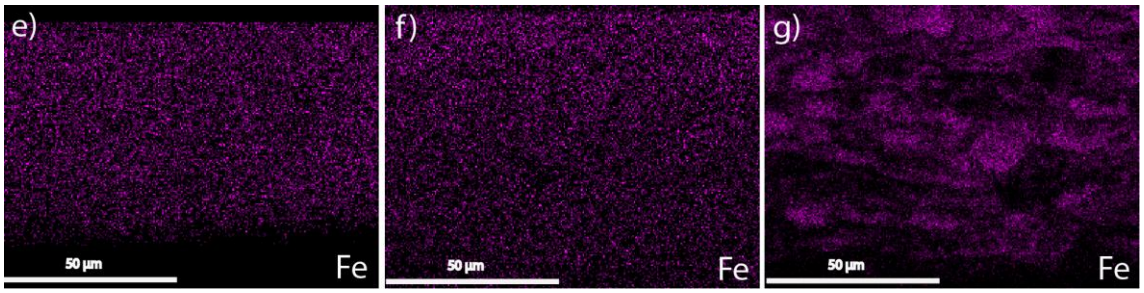

Figure 3. Cross-section images of neat carrageenan (a) and [Bmim][FeCl4]/Carrageenan blends with different IL contents: b) 10 wt. %, c) 20 wt.% and d) 40 wt.% of [Bmim][$FeCl_4$]. EDS images for the [Bmim][$FeCl_4$]/Carrageenan samples containing different IL contents: e) 10 wt.%, f) 20 wt.% and g) 40 wt.%

The presence of [Bmim][$FeCl_4$] into the carrageenan matrix was directly assessed by EDS analysis (Figure 3e)-g)). Independently of the IL content, all the hybrid samples present the chemical element of Iron (Fe) in their blends, identified by a purple colour. The EDS images shows a uniform [Bmim][$FeCl_4$] distribution along the polymer matrix for the 10 and 20 wt.% content samples, the 40 wt.% sample presenting a homogenous distribution of IL aggregates, confirming phase segregation of the filler for larger filler contents [33].

Physical-chemical, thermal and mechanical proprieties

Figure 4a) shows the FTIR-ATR spectra of the [Bmim][$FeCl_4$]/carrageenan samples.

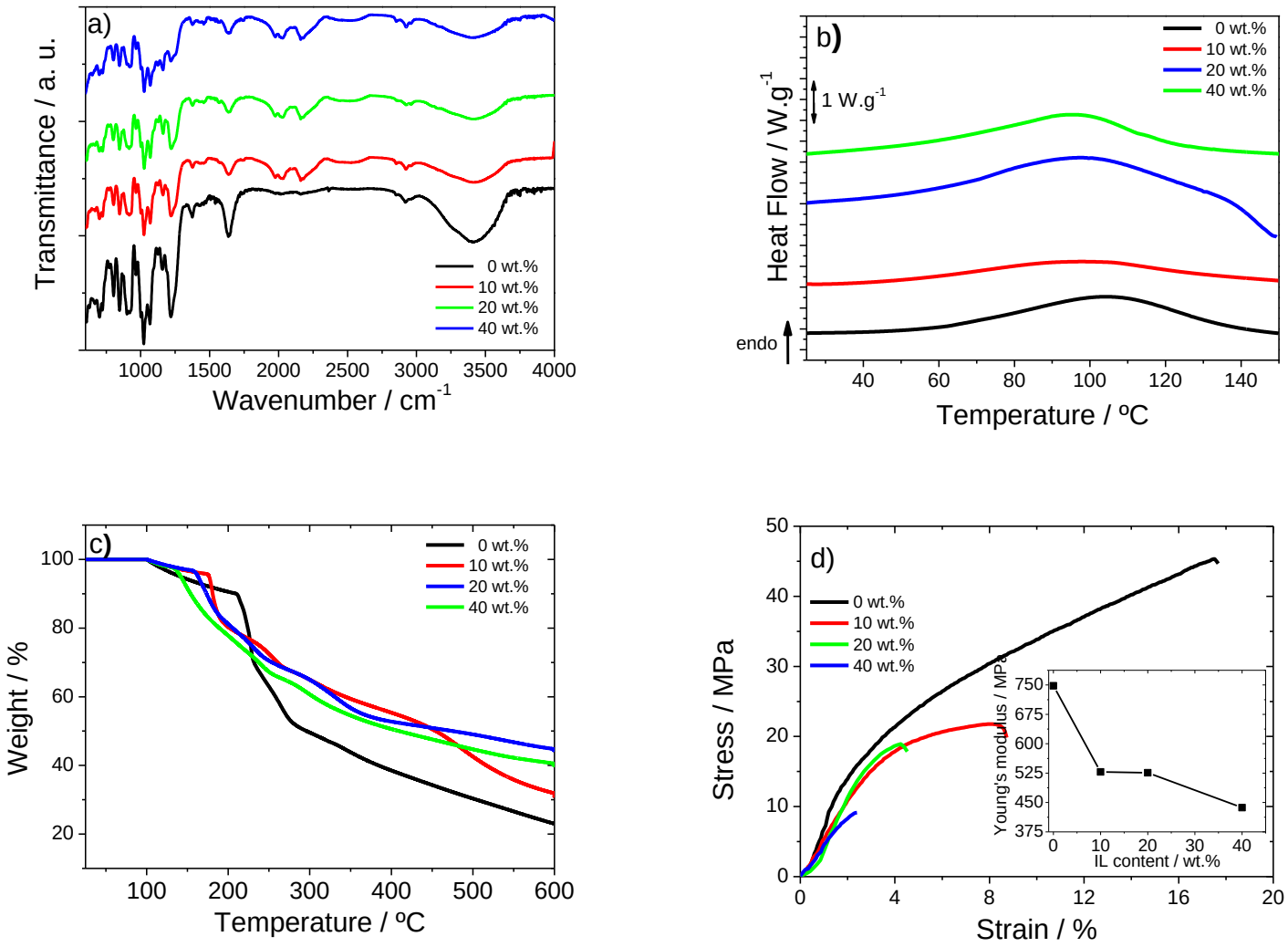

Figure 4. a) FTIR-ATR spectra, b) DSC scans, c) TGA thermograms and d) stress-strain mechanical curves for neat carrageenan and [Bmim][$FeCl_4$]/carrageenan samples containing different IL contents (insert: Young Modulus variation as a function of IL content).

The main characteristic absorption bands of neat carrageenan are observed in Figure 4a and presented in Table 1.

Table 1. FTIR peaks associated to carrageenan polymer [34-35].

Wavenumber (cm^{-1})	Assignments
3400	- O-H Stretching
1635	- C=O asymmetric stretch/N-H deformation
1240-1260	- S=O bond of sulphate esters
970-975	- Galactose groups
930-1070	- C-O of 3,6 anhydrogalactose
905	- C_2-O-SO_3 of 3,6-anhydrogalactose in C6
845	- C_2-O-SO_3 of 3,6-anhydrogalactose in C4
805	- C_2-O-SO_3 of 3,6-anhydrogalactose in C2

It is verified that the characteristic bands of carrageenan do not suffer relevant variations with the inclusion of the IL and no new bands appear, excepting the C–C and C–N stretching vibrations characteristics of the IL [Bmim][$FeCl_4$], attributed to the skeleton vibrations of the imidazolium ring of the cation at 1564 and 1450 cm^{-1} [36].

The DSC thermograms of neat carrageenan and the [Bmim][$FeCl_4$]/carrageenan blends are shown in Figure 4b). Independently of being the neat polymer or the [Bmim][$FeCl_4$]/carrageenan blends with different IL contents, just a single endothermic peak is observed between 70 and 130 ºC, corresponding to the glass transition temperature (Tg) of carrageenan with contribution of the intrinsic water within the samples [26].

The thermal stability of the samples is shown in the TGA thermograms of figure 4c). For neat carrageenan, three weigh loss degradation steps are observed. The weight loss occurs between 25-100ºC being attributed to the adsorbed and bound water loss [37]. The carrageenan polymeric backbone degradation occurs in the temperature range of 210 and 330 ºC [38] and the last degradation stage with a T_{onset} of ~750 ºC is attributed also to the last stage of carrageenan decomposition [38]. Independently of the [Bmim][$FeCl_4$] content, a decrease in the thermal stability is observed in the second and third steps, decreasing the blends stability with increasing IL content up to 40 wt.%. Further, the weight loss

related to the IL [Bmim][$FeCl_4$] decomposition occurs at approximately ~330 ºC in a single step and is ascribed to thermal decomposition through dealkylation [39].

The influence of the IL content into the mechanical properties of the blends was evaluated by stress-strain tensile measurements and the results are presented in figure 4d. Neat carrageenan shows the typical mechanical behaviour of a thermoplastic polymer [40], characterized by elastic and plastic regions separated by yielding. The incorporation of IL affects the mechanical behaviour proportional to the IL content. Figure 4d) shows that the plastic region and the maximum deformation of the blends decrease with increasing IL content. The insert of figure 4d shows the Young Modulus for the different [Bmim][$FeCl_4$]/ carrageenan blends obtained from the linear regime of the stress-strain curve at 2% of maximum elongation using the tangent method. All hybrid samples show a significant reduction of the Young Modulus with respect to the neat polymer, the reduction being larger to the 40 wt.% blend (Figure 4d).

Ionic conductivity

The ionic conductivity of the samples is presented in Figure 5. Figure 5a shows the typical Nyquist profiles at two temperatures 30 and 60 ºC for the [Bmim][$FeCl_4$] /Carrageenan sample incorporating 20 wt.%. Similar results are obtained for the samples with 10 and 40 wt.% of IL.

The Nyquist plots of Figure 5a are characterized by a semi-circle located in the high frequency range that corresponds to charge transfer process, the transition between high and low frequencies and a straight line at lower frequencies that is characteristic of charge diffusion process [41]. This behavior is dependent on IL content and temperature and it is observed that the semicircle represented in the figure 5a decreases with increasing of IL

content and temperature due to the decrease of the bulk resistance, i.e., increase in the number of charge carriers and mobility.

Figure 5b shown the ionic conductivity obtained from Nyquist plots as a function of temperature.

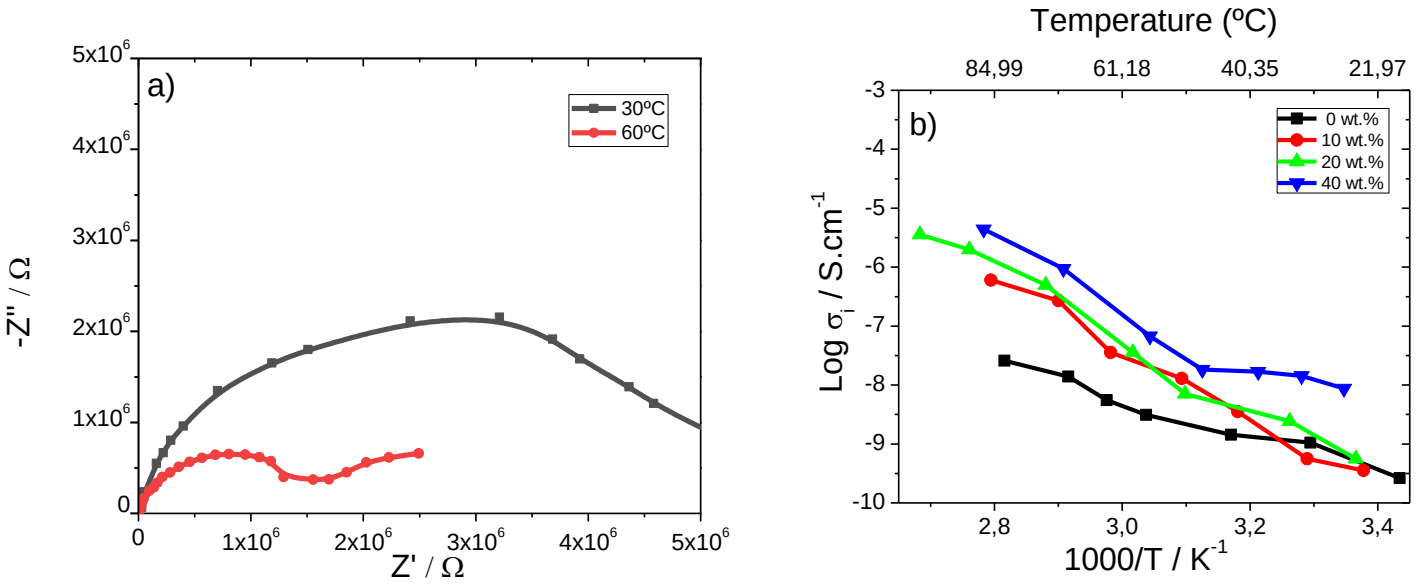

Figure 5. a) Nyquist plot for the 20 wt.% IL blend at 30 and 60 ºC and b) Arrhenius conductivity plots for [Bmim][$FeCl_4$]/carrageenan blends with different IL contents.

Figure 5b) shows the Arrhenius plots of the ionic conductivity at temperatures ranging from 20 to 95 ºC. The ionic conductivity of carrageenan blends increases with IL incorporation into the polymer matrix and with increasing IL content, as a result of the higher number of ionic positive and negative charges from the IL into the carrageenan matrix and their increased mobility [42]. Moreover, the value of the ionic conductivity also increases with increasing temperature, as higher temperatures promote the mobility of the segmental motion of the polymer chains, supporting mobility of the ionic species [43]. At room temperature, the highest ionic conductivity is 8.74×10^{-9} S/cm for the composite with 40 wt.% IL content, as compared with 3.3×10^{-11} for the neat polymer. It is to notice that the ionic conductivity value obtained with the [Bmim][$FeCl_4$] IL is lower when

compared to the one obtained with other IL´s, such as [Ch][DHP] IL, for samples with 40% w/w IL content (1.2×10^{-6} S/cm) [32], being nevertheless suitable for piezoresistive sensing applications, as demonstrated in the following.

Piezoresistive pressure sensor

The suitability of the developed [Bmim][$FeCl_4$]/carrageenan samples to be applied as pressure sensors was evaluated. Figure 6a-b) shows the results of the graphical user interface (GUI) by colormap chart for the sample with 40 wt.% IL content where the red and blue colours represent high and low pressure, respectively. The electronic systems starts by calibrating the initial position of all matrix sensors. Thus, in the relaxed state (no pressure applied) all the sensors read the same value. When a pressure force is applied to the device, the sensors in the matrix detect the variation of the applied force and output the data mapping the location where the pressure was applied as well as the value of the specific pressure. Figure 6a) shows the pressure distribution for a mass of 200 g.

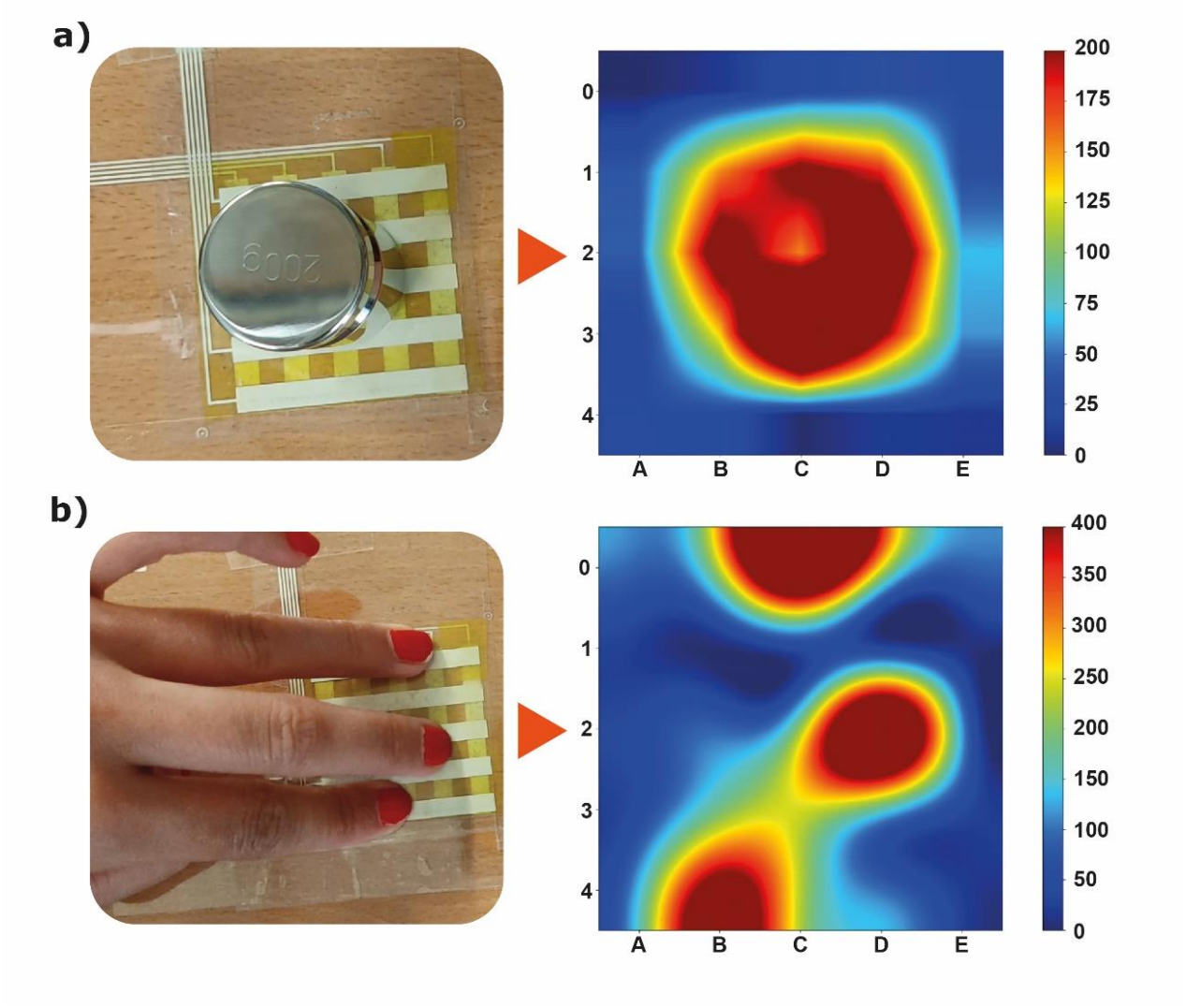

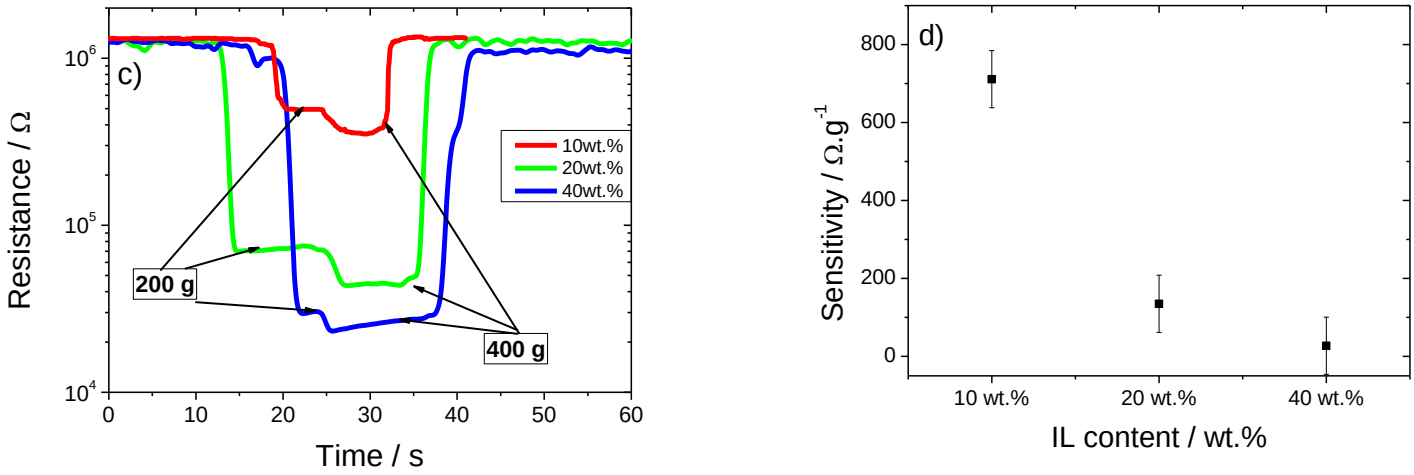

Figure 6. a) Image of the 200g weight on top of the sensing device, b) multi finger pressure detection on the 5x5 matrix, c) resistance variation for weights of 200 g and 400 g placed on devices (position 2C of the matrix) fabricates with hybrid films with filler

concentrations of 10, 20 and 40 % and d) sensor sensitivity calculated from the 200 g to 400 g sensor response variations.

In Figure 6b) a simultaneous multiple finger pressure detection is shown (position 0C, 2D and 4B at the same time) showing the multitouch capability of the device with no relevant cross-talk.

Figure 6c shows the time response of the different sensors when first a weight of 200 g and then a weight of 400 g is placed on devices developed with the different blends.

Figure 6d represents the sensitivity (variation of the resistance as a function of weight) for all [Bmim][$FeCl_4$]/carrageenan blends. It is observed that the sensitivity value decreases with increasing the IL content, as the mechanically induced variations of the ionic conductivity are lower for higher ionic conductivity values.

Thus, it is shown that both the initial sensor resistance and the sensor sensitivity can be tuned by controlling the IL concentration, allowing to tune the sensor for specific applications and/or electronic systems.

Recyclability and reuse of the sensing materials

As carrageenan is a natural polymer and attending to the sustainability and circular economy paradigms [44], the possibility to recycle the developed materials was evaluated. For this purpose, the [Bmim][$FeCl_4$]/carrageenan sample with 20 wt.% IL content was selected as representative sample as it presents resistance and sensibility values comprised between the ones obtained for the other two IL contents.

The samples were recycled as indicated in the experimental section (Figure 1). The mechanical properties of the recycled sample (Figure 7a) show a similar behaviour to the original ones, showing just a reduction in a tensile strength, with a slight decrease in the Young Modulus from 526 MPa to 488 MPa for the reused sample.

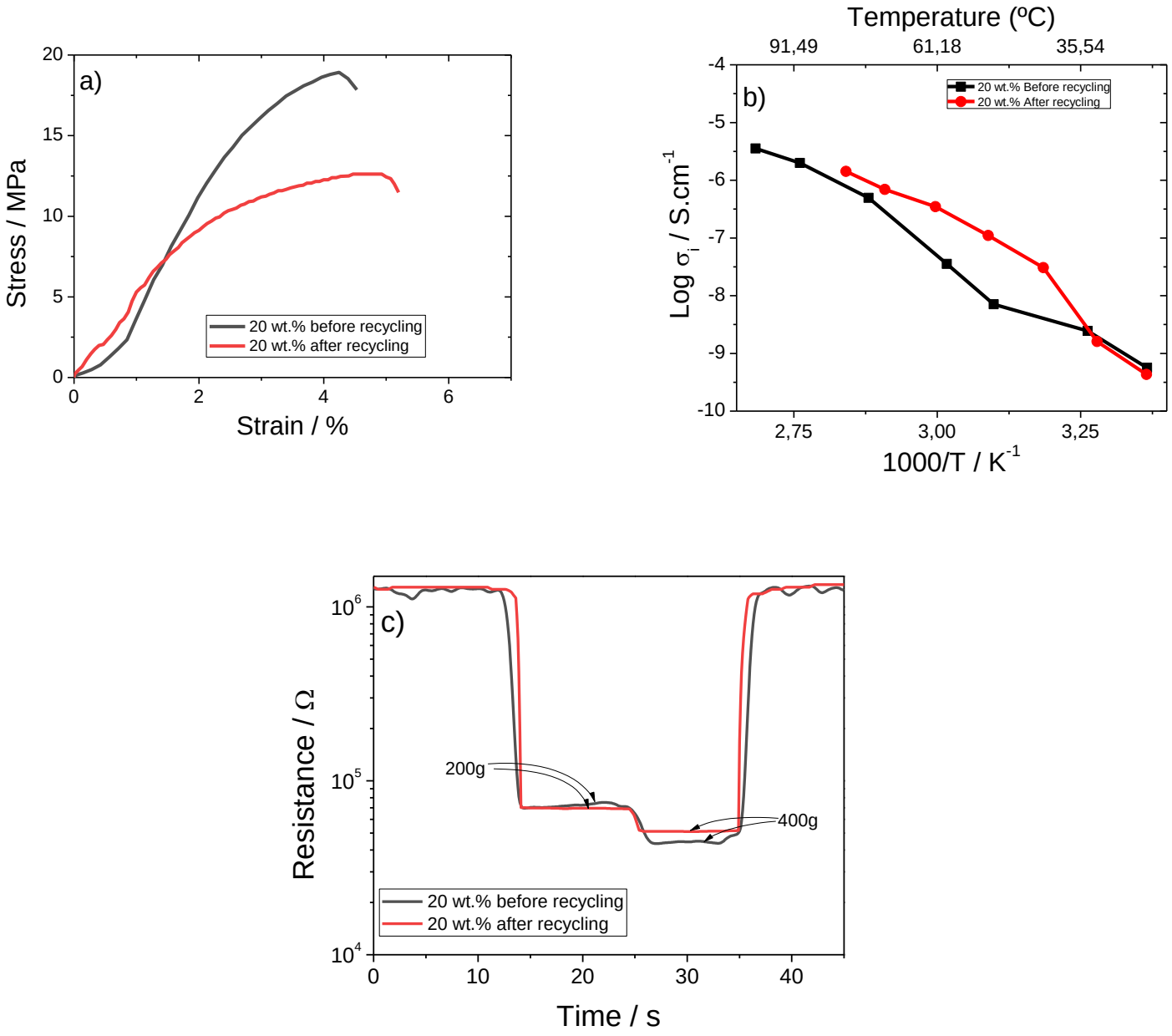

Figure 7. a) Mechanical response and b) Arrhenius conductivity plot for neat and recycled [Bmim][$FeCl_4$]/carrageenan blends with 20 wt. % IL content. c) Resistance variation when a weight of 200 g first and then a weight of 400 g were placed on a device developed with neat and recycled [Bmim][$FeCl_4$]/carrageenan blends with 20 wt. % IL content.

With respect to the ionic conductivity, it is the same for the original and the recycled sample at room temperature, being the slightly higher for the recycled sample than for the

original one for temperatures above ~35 ºC (Figure 7b). In addition, the ionic conductivity value increases with increasing temperature (Figure 7b). The slightly higher ionic conductivity obtained for the recycled blend comparatively to the original one indicates that some water molecules may have been adsorbed in the recycled carrageenan sample, which are thermally activated, contributing to the increase of the electrical conductivity upon heating.

The potential to further develop a pressure sensor after the recycling process of the [Bmim][$FeCl_4$]/carrageenan blend was also evaluated. Figure 7c) shows the variation of the resistance of the [Bmim][$FeCl_4$]/carrageenan blend with 20% IL before and after the recycling process, leading to no relevant variations in the operation of the developed sensing devices.

In the developed application just the [Bmim][$FeCl_4$]/carrageenan blend was recycled and the electronic components (electrodes and substrates) maintained for all tests.

As shown in Figure 7c), the recycled blend is sensible to the placement of the 200 g and 400 g, with no significant differences being observed in the sensing device response when prepared either with as processed or recycled [Bmim][$FeCl_4$]/carrageenan samples, successfully demonstrating the proper functional response of the recycles samples and their contribution towards more sustainable sensor and electronic systems.

CONCLUSIONS

Carrageenan film blends with different [Bmim][$FeCl_4$] Il contents were prepared by a solvent casting method at room temperature aiming to provide sustainable sensing materials compatible with circular economy considerations. The incorporation of the IL within the polymer matrix induces changes in the morphology of the blends, leading to more compact samples with well dispersed and distributed IL, excepting for the sample

with the highest IL content (40 wt%) which shows phase segregation of the IL within the polymer matrix. No significant changes occur in the chemical properties of the developed blends, however the thermal stability decreases with the incorporation of the IL within the carrageenan matrix. The mechanical properties are dependent on IL content, the Young modulus of the samples decreasing from 748 MPa for neat carrageenan to 437 MPa for the sample comprising 40 %wt. of IL. Independently of the IL content, a decrease in resistance occurs with increasing temperature from 30 to 60 ºC, increasing the IL conductivity with increasing IL content from 3.3×10^{-11} S/cm for the neat polymer up to 8.74×10^{-9} S/cm for the [Bmim][$FeCl_4$]/carrageenan blends with 40 wt.% filler content. The recyclability of the developed samples was accessed being observed no significant changes in mechanical and electrical properties. The performance of both neat and recycled blends to be used as printable pressure sensors was demonstrated being the sensor resistance response and sensitivity (711 to 27 Ω/g) tuned by the IL concentration.

AUTHOR INFORMATION

Corresponding Authors

cmscosta@fisica.uminho.pt (Carlos M. Costa),

senentxu.lanceros@bcmaterials.net (Senentxu Lanceros-Méndez)

Author Contributions

João P. Serra and Nelson Pereira contributed equally to this paper. The manuscript was written through contributions of all authors. All authors have given approval to the final version of the manuscript

Notes

The authors declare no competing financial interest.

ACKNOWLEDGEMENTS

The authors thank financial support from the Fundação para a Ciência e Tecnologia (FCT): Strategic Funding grants UIDB/04650/2020, UID/FIS/04650/2020, UID/EEA/04436/2020, and UID/QUI/0686/2020; projects POCI-01-0145-FEDER-028157 and PTDC/FIS-MAC/ 28157/2017; grants 2021.08158.BD (J.P.S), SFRH/BPD/121526/2016 (D.M.C) and 2020.04028.CEECIND (C.M.C.). Financial support from the Basque Government Industry Department under the ELKARTEK program is also acknowledged, as well as technical and human support provided by SGIker (UPV/EHU/ ERDF, EU).

REFERENCES

1. Singh, R. P.; Javaid, M.; Haleem, A.; Suman, R. Internet of Things (Iot) Applications to Fight against Covid-19 Pandemic. *Diabetes & Metabolic Syndrome: Clinical Research & Reviews* **2020,** *14*, 521-524, https://doi.org/10.1016/j.dsx.2020.04.041.

2. Ghosh, A.; Chakraborty, D.; Law, A. Artificial Intelligence in Internet of Things. *CAAI Transactions on Intelligence Technology* **2018,** *3*, 208-218, https://doi.org/10.1049/trit.2018.1008.

3. Li, S.; Da Xu, L.; Zhao, S. 5g Internet of Things: A Survey. *Journal of Industrial Information Integration* **2018,** *10*, 1-9, https://doi.org/10.1016/j.jii.2018.01.005.

4. Zanella, A.; Bui, N.; Castellani, A.; Vangelista, L.; Zorzi, M. Internet of Things for Smart Cities. *IEEE Internet of Things journal* **2014,** *1*, 22-32, DOI: 10.1109/JIOT.2014.2306328.

5. Borgia, E. The Internet of Things Vision: Key Features, Applications and Open Issues. *Computer Communications* **2014,** *54*, 1-31, https://doi.org/10.1016/j.comcom.2014.09.008.

6. Jin, J.; Gubbi, J.; Marusic, S.; Palaniswami, M. An Information Framework for Creating a Smart City through Internet of Things. *IEEE Internet of Things journal* **2014,** *1*, 112-121.

7. Wang, X.; Yu, J.; Cui, Y.; Li, W. Research Progress of Flexible Wearable Pressure Sensors. *Sensors and Actuators A: Physical* **2021,** *330*, 112838, https://doi.org/10.1016/j.sna.2021.112838.

8. Su, Y.; Zheng, L.; Yao, D.; Zhang, X.; Chen, H.; Xu, H. Robust Physiological Signal Monitoring by a Flexible Piezoresistive Sensor Microstructured with

Filamentating Laser Pulses. *Sensors and Actuators A: Physical* **2021,** 112907, https://doi.org/10.1016/j.sna.2021.112907.

9. Chen, S.; Bai, C.; Zhang, C.; Geng, D.; Liu, R.; Xie, Y.; Zhou, W. Flexible Piezoresistive Three-Dimensional Force Sensor Based on Interlocked Structures. *Sensors and Actuators A: Physical* **2021,** 112857, https://doi.org/10.1016/j.sna.2021.112857.

10. Fiorillo, A. S.; Critello, C. D.; Pullano, S. A. Theory, Technology and Applications of Piezoresistive Sensors: A Review. *Sensors and Actuators A: Physical* **2018,** *281*, 156-175, https://doi.org/10.1016/j.sna.2018.07.006.

11. Jung, Y.; Jung, K. K.; Kim, D. H.; Kwak, D. H.; Ahn, S.; Han, J. S.; Ko, J. S. Flexible and Highly Sensitive Three-Axis Pressure Sensors Based on Carbon Nanotube/Polydimethylsiloxane Composite Pyramid Arrays. *Sensors and Actuators A: Physical* **2021,** 113034, https://doi.org/10.1016/j.sna.2021.113034.

12. Yan, J.; Ma, Y.; Li, X.; Zhang, C.; Cao, M.; Chen, W.; Luo, S.; Zhu, M.; Gao, Y. Flexible and High-Sensitivity Piezoresistive Sensor Based on Mxene Composite with Wrinkle Structure. *Ceramics International* **2020,** *46*, 23592-23598, https://doi.org/10.1016/j.ceramint.2020.06.131.

13. Ma, Z.; Wei, A.; Li, Y.; Shao, L.; Zhang, H.; Xiang, X.; Wang, J.; Ren, Q.; Kang, S.; Dong, D. Lightweight, Flexible and Highly Sensitive Segregated Microcellular Nanocomposite Piezoresistive Sensors for Human Motion Detection. *Composites Science and Technology* **2021,** *203*, 108571, https://doi.org/10.1016/j.compscitech.2020.108571.

14. Ricohermoso, E.; Rosenburg, F.; Klug, F.; Nicoloso, N.; Schlaak, H. F.; Riedel, R.; Ionescu, E. Piezoresistive Carbon-Containing Ceramic Nanocomposites – a Review. *Open Ceramics* **2021,** *5*, 100057, https://doi.org/10.1016/j.oceram.2021.100057.

15. He, J.; Zhang, Y.; Zhou, R.; Meng, L.; Chen, T.; Mai, W.; Pan, C. Recent Advances of Wearable and Flexible Piezoresistivity Pressure Sensor Devices and Its

Future Prospects. *Journal of Materiomics* **2020,** *6*, 86-101, https://doi.org/10.1016/j.jmat.2020.01.009.

16. Ma, Y.; Liu, N.; Li, L.; Hu, X.; Zou, Z.; Wang, J.; Luo, S.; Gao, Y. A Highly Flexible and Sensitive Piezoresistive Sensor Based on Mxene with Greatly Changed Interlayer Distances. *Nature communications* **2017,** *8*, 1-8, https://doi.org/10.1038/s41467-017-01136-9.

17. Costa, P.; Silvia, C.; Viana, J. C.; Lanceros Mendez, S. Extruded Thermoplastic Elastomers Styrene–Butadiene–Styrene/Carbon Nanotubes Composites for Strain Sensor Applications. *Composites Part B: Engineering* **2014,** *57*, 242-249, https://doi.org/10.1016/j.compositesb.2013.10.006.

18. Dong, K.; Liu, X.; Dong, H.; Zhang, X.; Zhang, S. Multiscale Studies on Ionic Liquids. *Chemical Reviews* **2017,** *117*, 6636-6695, https://doi.org/10.1021/acs.chemrev.6b00776.

19. Singh, S. K.; Savoy, A. W. Ionic Liquids Synthesis and Applications: An Overview. *Journal of Molecular Liquids* **2020,** *297*, 112038, https://doi.org/10.1016/j.molliq.2019.112038.

20. Correia, D. M.; Fernandes, L. C.; Martins, P. M.; García-Astrain, C.; Costa, C. M.; Reguera, J.; Lanceros-Méndez, S. Ionic Liquid–Polymer Composites: A New Platform for Multifunctional Applications. *Advanced Functional Materials* **2020,** *30*, 1909736, https://doi.org/10.1002/adfm.201909736.

21. Fernandes, L. C.; Correia, D. M.; Pereira, N.; Tubio, C. R.; Lanceros-Méndez, S. Highly Sensitive Transparent Piezoionic Materials and Their Applicability as Printable Pressure Sensors. *Composites Science and Technology* **2021,** *214*, 108976, https://doi.org/10.1016/j.compscitech.2021.108976.

22. Halonen, N.; Pálvölgyi, P. S.; Bassani, A.; Fiorentini, C.; Nair, R.; Spigno, G.; Kordas, K. Bio-Based Smart Materials for Food Packaging and Sensors – a Review. *Frontiers in Materials* **2020,** *7*, 82, https://doi.org/10.3389/fmats.2020.00082.

23. Nazari, F.; Ghoreishi, S. M.; Khoobi, A. Bio-Based Fe3o4/Chitosan Nanocomposite Sensor for Response Surface Methodology and Sensitive Determination of Gallic Acid. *International Journal of Biological Macromolecules* **2020,** *160*, 456-469, https://doi.org/10.1016/j.ijbiomac.2020.05.205.

24. Wang, G.; Zhang, Q.; Wang, Q.; Zhou, L.; Gao, G. Bio-Based Hydrogel Transducer for Measuring Human Motion with Stable Adhesion and Ultrahigh Toughness. *ACS Applied Materials & Interfaces* **2021,** *13*, 24173-24182, https://doi.org/10.1021/acsami.1c05098.

25. van de Velde, F. Structure and Function of Hybrid Carrageenans. *Food Hydrocolloids* **2008,** *22*, 727-734, https://doi.org/10.1016/j.foodhyd.2007.05.013.

26. Moniha, V.; Alagar, M.; Selvasekarapandian, S.; Sundaresan, B.; Hemalatha, R.; Boopathi, G. Synthesis and Characterization of Bio-Polymer Electrolyte Based on Iota-Carrageenan with Ammonium Thiocyanate and Its Applications. *Journal of Solid State Electrochemistry* **2018,** *22*, 3209-3223, https://doi.org/10.1007/s10008-018-4028-6.

27. Sugumaran, T.; Silvaraj, D.; mohamad saidi, N.; Farhana, N.; T subramaniam, R.; Kasi, R. The Conductivity and Dielectric Studies of Polymer Electrolytes Based on Iota-Carrageenan with Sodium Iodide and 1-Butyl-3-Methylimidazolium Iodide for the Dye-Sensitized Solar Cells. *Ionics* **2019,** *25*, 763-771, https://doi.org/10.1007/s11581-018-2756-3.

28. Soleimani, F.; Sadeghi, M.; Shahsavari, H. Preparation and Swelling Behavior of Carrageenan-Graft-Polymethacrylamide Superabsorbent Hydrogel as a Releasing Drug

System. *Indian Journal of Science and Technology* **2012,** *5*, 2143-2147, DOI: 10.17485/ijst/2012/v5i2.18.

29. Jayaramudu, T.; Raghavendra, G. M.; Varaprasad, K.; Sadiku, R.; Ramam, K.; Raju, K. M. Iota-Carrageenan-Based Biodegradable Ag0 Nanocomposite Hydrogels for the Inactivation of Bacteria. *Carbohydrate polymers* **2013,** *95*, 188-194, https://doi.org/10.1016/j.carbpol.2013.02.075.

30. Satoshi, H.; Hiro-o, H. Discovery of a Magnetic Ionic Liquid [Bmim]Fecl4. *Chemistry Letters* **2004,** *33*, 1590-1591, https://doi.org/10.1246/cl.2004.1590.

31. Ghani, N. A. A.; Anuar, F. H.; Ahmad, A.; Mobarak, N. N.; Shamsudin, I. J.; Dzulkipli, M. Z.; Hassan, N. H. Incorporating 1-Butyl-3-Methylimidazolium Chloride Ionic Liquid into Iota Carrageenan Solid Biopolymer Electrolyte for Electrochemical Devices Application. *Sains Malaysiana* **2020,** *49*, 305-313, http://dx.doi.org/10.17576/jsm-2020-4902-08.

32. Serra, J. P.; Fernandes, L. C.; Correia, D. M.; Tubio, C. R.; Vilas-Vilela, J. L.; Tariq, M.; Esperança, J. M. S. S.; Costa, C. M.; Lanceros-Mendez, S. Environmentally Friendly Carrageenan-Based Ionic-Liquid Driven Soft Actuators. *Materials Advances* **2022,** *3*, 937-945, https://doi.org/10.1039/D1MA00887K.

33. Lipatov, Y. S.; Nesterov, A. E.; Ignatova, T. D.; Nesterov, D. A. Effect of Polymer–Filler Surface Interactions on the Phase Separation in Polymer Blends. *Polymer* **2002,** *43*, 875-880, https://doi.org/10.1016/S0032-3861(01)00632-2.

34. Pereira, L.; Amado, A. M.; Critchley, A. T.; Van de Velde, F.; Ribeiro-Claro, P. J. Identification of Selected Seaweed Polysaccharides (Phycocolloids) by Vibrational Spectroscopy (Ftir-Atr and Ft-Raman). *Food Hydrocolloids* **2009,** *23*, 1903-1909, https://doi.org/10.1016/j.foodhyd.2008.11.014.

35. Rajasulochana, N. G. Analysis on the Seasonal Variations in Carrageenans of Hypnea Flagelliformis and Sarconema Filiforme by Ftir Spectroscopy. *Asian Journal of Chemistry.* **2009,** *21*, 4547-4552, https://asianjournalofchemistry.co.in/user/journal/viewarticle.aspx?ArticleID=21_6_60.

36. Xie, Z.-L.; Jelicic, A.; Wang, F.-P.; Rabu, P.; Friedrich, A.; Beuermann, S.; Taubert, A. Transparent, Flexible, and Paramagnetic Ionogels Based on Pmma and the Iron-Based Ionic Liquid 1-Butyl-3-Methylimidazolium Tetrachloroferrate(Iii) Bmim Fecl4. *Journal of Materials Chemistry* **2010,** *20*, 9543-9549, https://doi.org/10.1039/C0JM01733G.

37. Sadeghi, M. Synthesis of a Biocopolymer Carrageenan-G-Poly(Aam-Co-Ia)/Montmorilonite Superabsorbent Hydrogel Composite. *Brazilian Journal of Chemical Engineering* **2012,** *29*, 295-305, https://doi.org/10.1590/S0104-66322012000200010.

38. Jumaah, F. N.; Mobarak, N. N.; Ahmad, A.; Ghani, M. A.; Rahman, M. Y. A. Derivative of Iota-Carrageenan as Solid Polymer Electrolyte. *Ionics* **2015,** *21*, 1311-1320, https://doi.org/10.1007/s11581-014-1306-x.

39. Zhou, C.; Yu, X.; Ma, H.; Huang, X.; Zhang, H.; Jin, J. Properties and Catalytic Activity of Magnetic and Acidic Ionic Liquids: Experimental and Molecular Simulation. *Carbohydrate Polymers* **2014,** *105*, 300-307, https://doi.org/10.1016/j.carbpol.2014.01.071.

40. Costa, C. M.; Sencadas, V.; Pelicano, I.; Martins, F.; Rocha, J. G.; Lanceros-Méndez, S. Microscopic Origin of the High-Strain Mechanical Response of Poled and Non-Poled Poly (Vinylidene Fluoride) in the B-Phase. *Journal of non-crystalline solids* **2008,** *354*, 3871-3876, https://doi.org/10.1016/j.jnoncrysol.2008.05.008.

41. Park, M.; Zhang, X.; Chung, M.; Less, G. B.; Sastry, A. M. A Review of Conduction Phenomena in Li-Ion Batteries. *Journal of Power Sources* **2010,** *195*, 7904-7929, https://doi.org/10.1016/j.jpowsour.2010.06.060.

42. Leones, R.; Costa, C.; Machado, A.; Esperança, J.; Silva, M. M.; Lanceros-Méndez, S. Development of Solid Polymer Electrolytes Based on Poly (Vinylidene Fluoride-Trifluoroethylene) and the [N1 1 1 2 (Oh)][Ntf2] Ionic Liquid for Energy Storage Applications. *Solid State Ionics* **2013,** *253*, 143-150, https://doi.org/10.1016/j.ssi.2013.09.042.

43. Leones, R.; Costa, C.; Machado, A.; Esperança, J.; Silva, M. M.; Lanceros-Méndez, S. Effect of Ionic Liquid Anion Type in the Performance of Solid Polymer Electrolytes Based on Poly (Vinylidene Fluoride-Trifluoroethylene). *Electroanalysis* **2015,** *27*, 457-464, https://doi.org/10.1002/elan.201400530.

44. Sgroi, M.; Vagliasindi, F. G. A.; Roccaro, P. Feasibility, Sustainability and Circular Economy Concepts in Water Reuse. *Current Opinion in Environmental Science & Health* **2018,** *2*, 20-25, https://doi.org/10.1016/j.coesh.2018.01.004.

TOC graphic

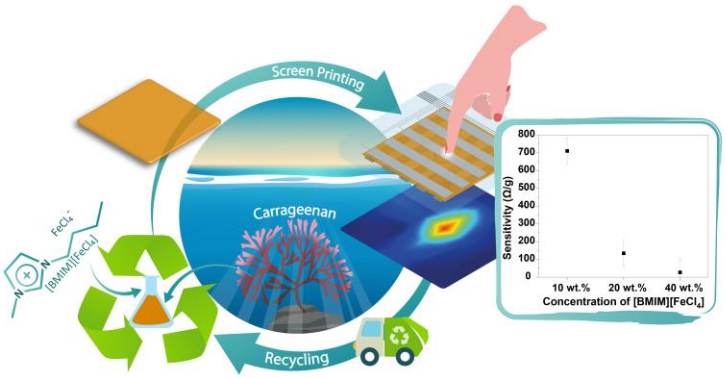

This work represents a novel blend based on carrageenan biopolymer and a ionic liquid, 1-butyl-3-methylimidazolium tetrachloroferrate ([Bmim][$FeCl_4$]) with focus on the recyclability and reuse for pressure sensor applications